## Supplementary Information for:

# An *in silico-in vitro* pipeline for drug cardiotoxicity screening identifies ionic proarrhythmia mechanisms

Alexander P. Clark, Siyu Wei, Darshan Kalola, Trine Krogh-Madsen, David J. Christini

---

**Table SI:** Percentage of current isolated

| Current | Best protocol isolation | Final protocol isolation |
|---|---|---|
| $I_{Kr}$ | 62% | 62% |
| $I_{CaL}$ | 91% | 93% |
| $I_{Na}$ | 91% | 89% |
| $I_{to}$ | 80% | 81% |
| $I_{K1}$ | 66% | 64% |
| $I_{f}$ | 51% | 50% |
| $I_{Ks}$ | 42% | 39% |

The best protocol isolation column shows the maximum current isolation for the protocols displayed in Figures S2-S8. The final protocol isolation column shows the maximum current isolation for the protocol used in experiments (Figure S9). This table shows that, once combined with 500 ms holding steps, there is little change in the current isolation. $I_{Ks}$ has the largest decrease in current isolation (7.1%), with all other currents changing by less than 5%.

**Table SII:** Simulated effect of extracellular calcium concentration on current isolation with the optimized VC protocol.

| Current | Current isolation at 1.2 mM | Current Isolation at 2 mM |
|---|---|---|
| $I_{Kr}$ | 63% | 62% |
| $I_{CaL}$ | 91% | 93% |
| $I_{Na}$ | 90% | 89% |
| $I_{to}$ | 80% | 81% |
| $I_{K1}$ | 65% | 64% |
| $I_f$ | 50% | 50% |
| $I_{Ks}$ | 40% | 39% |

The concentration of $Ca^{2+}$ in the patch-clamp experiments (2 mM) is unphysiologically large. To understand the effect of $Ca^{2+}$ concentration, we calculated the maximum current isolation in the Kernik-Clancy model with extracellular concentrations set to a physiologically normal $Ca^{2+}$ concentration (1.2 mM). The difference in percent isolation is very small between these two concentrations.

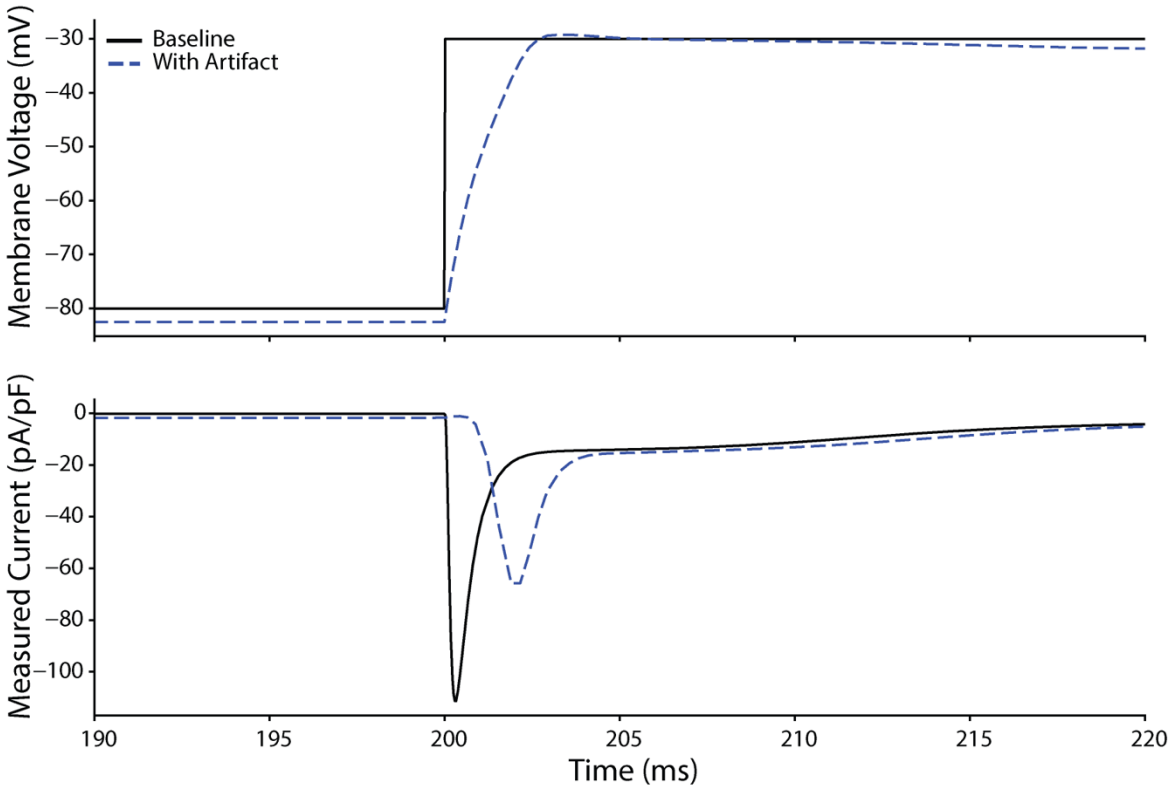


**Figure S1: The effect of experimental artifact on VC data designed to activate sodium channels.** The experimental artifact used in this simulation included a voltage offset of -2.8 mV, seal resistance of 1 GΩ, and access resistance of 20 MΩ. The top panel shows the voltage experienced by the cell (dashed blue) compared to the command voltage (black). The voltage offset shifts the membrane voltage negative by 2.8 mV, which has little effect on the current response. The relatively high access resistance is what causes the gradual slope upwards from the starting voltage of -80 mV to the ending voltage of -30 mV. This gradual slope in the membrane voltage leads to a delayed and reduced peak current (bottom) response.

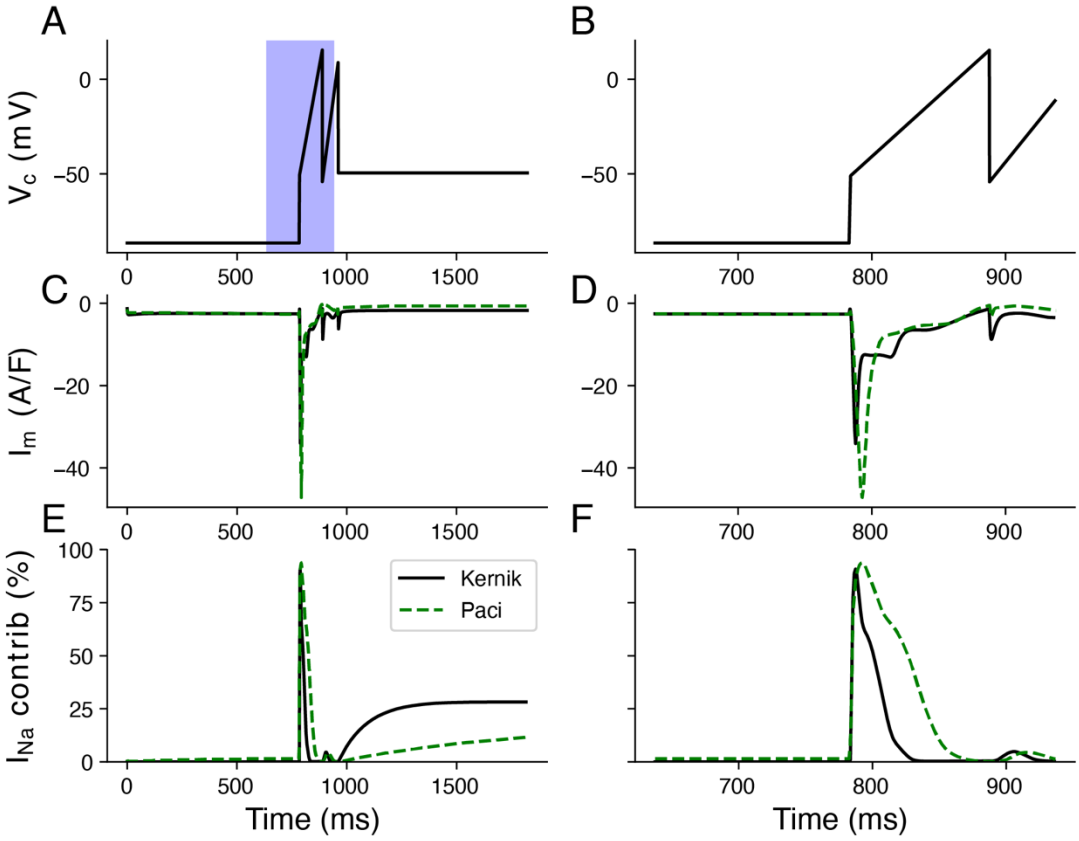


**Figure S2: The optimized protocol for $I_{Na}$ with Kernik-Clancy and Paci current response.** **A**, Optimized $I_{Na}$ protocol**.** The total current response (**C**) and $I_{Na}$ contribution (**E**) for both the Kernik-Clancy and Paci models. **B,** The portion of the protocol shaded in **A**, which includes the maximum $I_{Na}$ contribution. The total current response (**D**) and $I_{Na}$ contribution (**F**) for the portion of the protocol displayed in **B.**

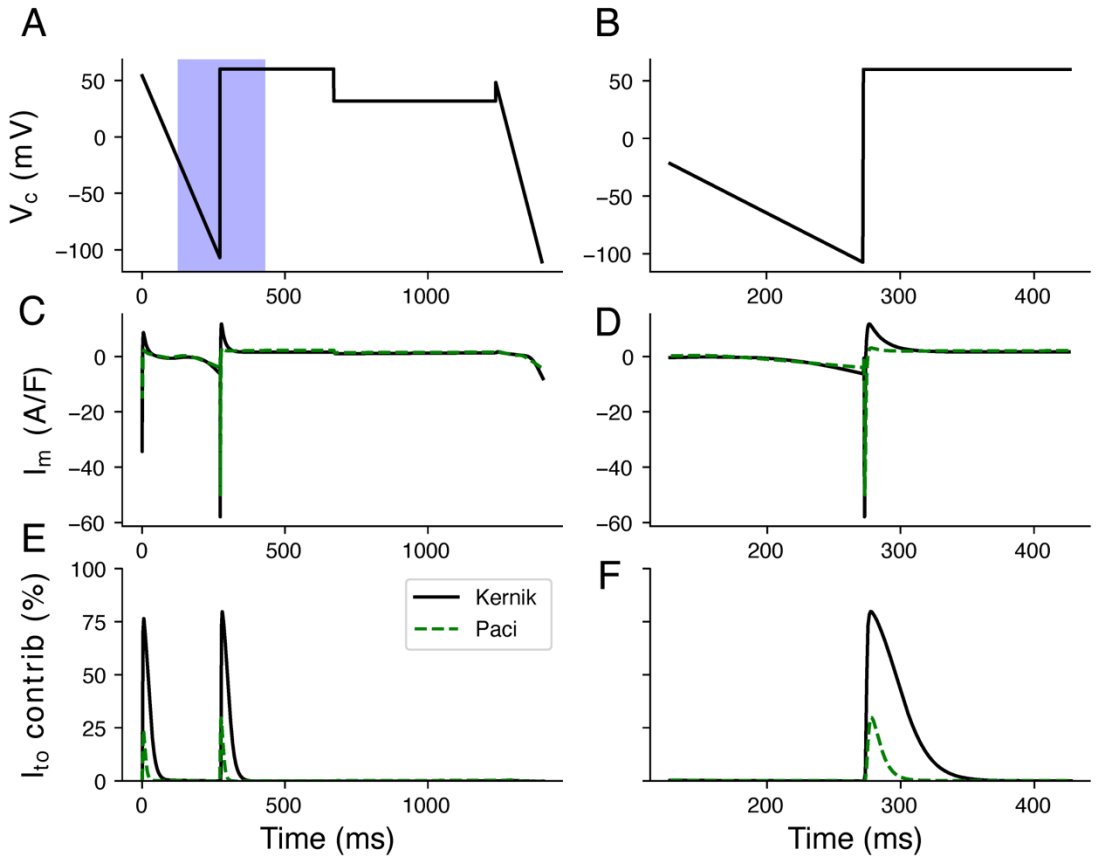


**Figure S3: The optimized protocol for $I_{to}$ with Kernik-Clancy and Paci current responses.**

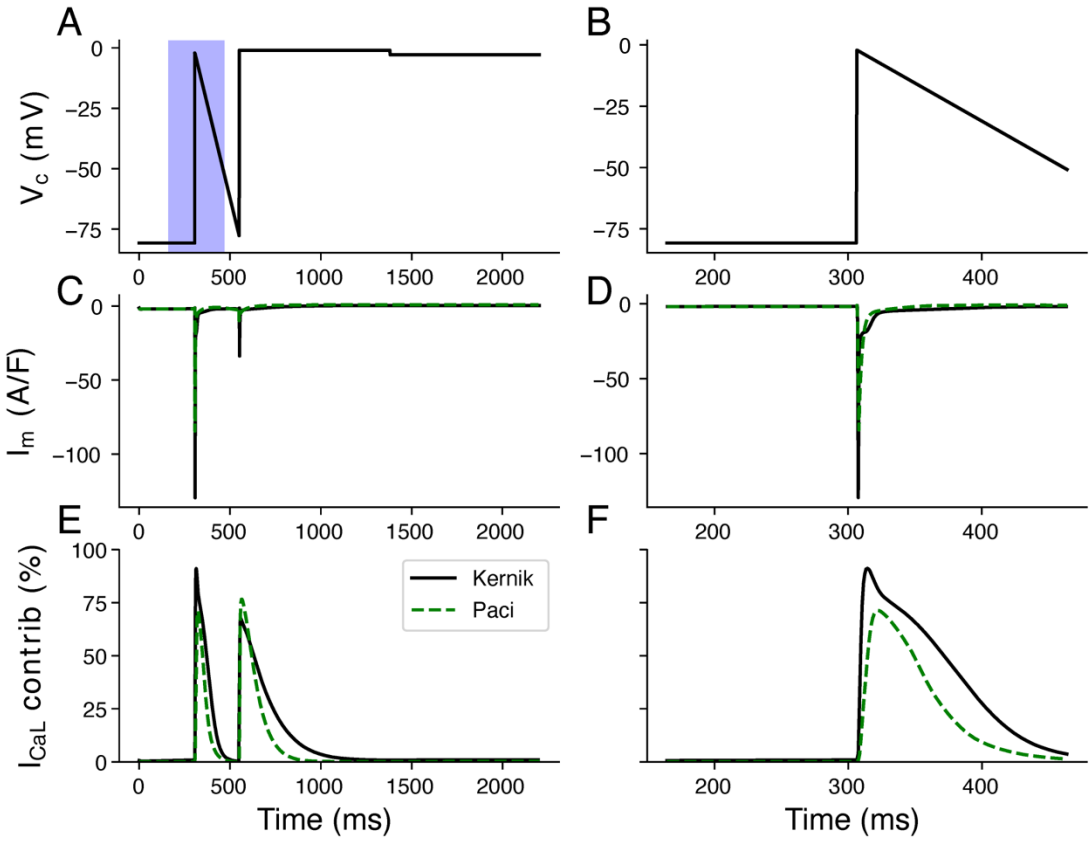


**Figure S4: The optimized protocol for $I_{CaL}$ with Kernik-Clancy and Paci current response.**

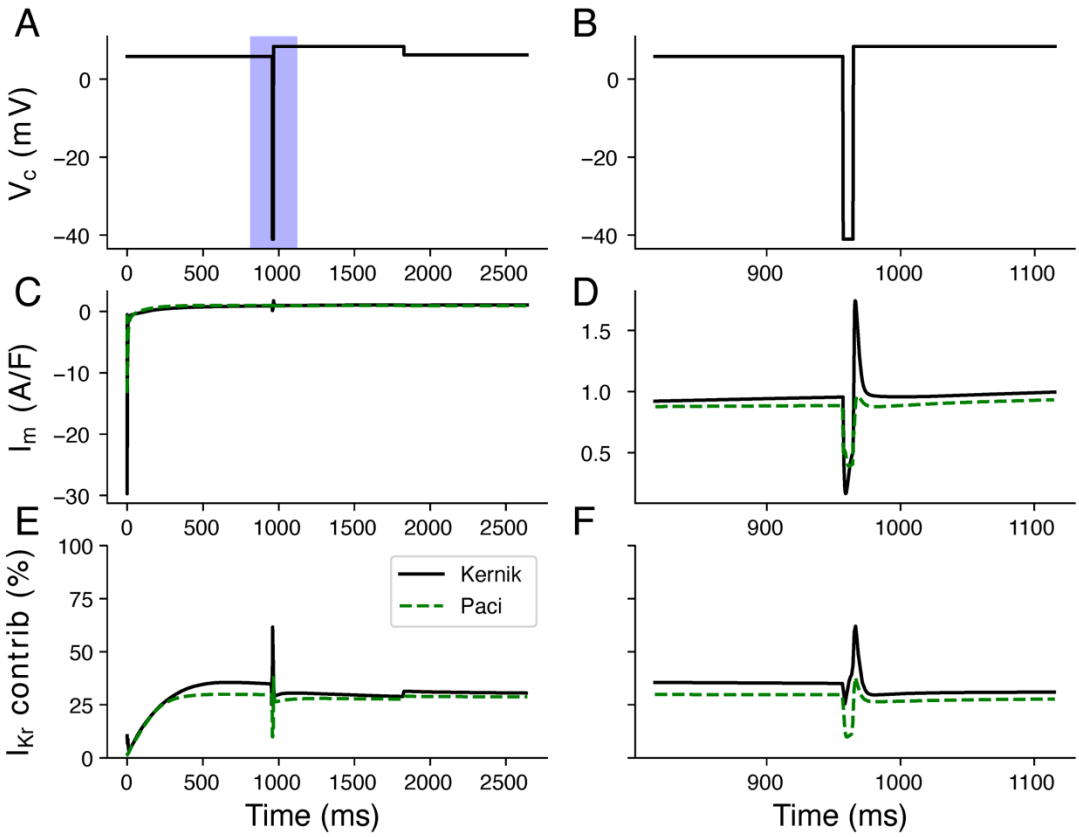


**Figure S5: The optimized protocol for $I_{Kr}$ with Kernik-Clancy and Paci current responses.**

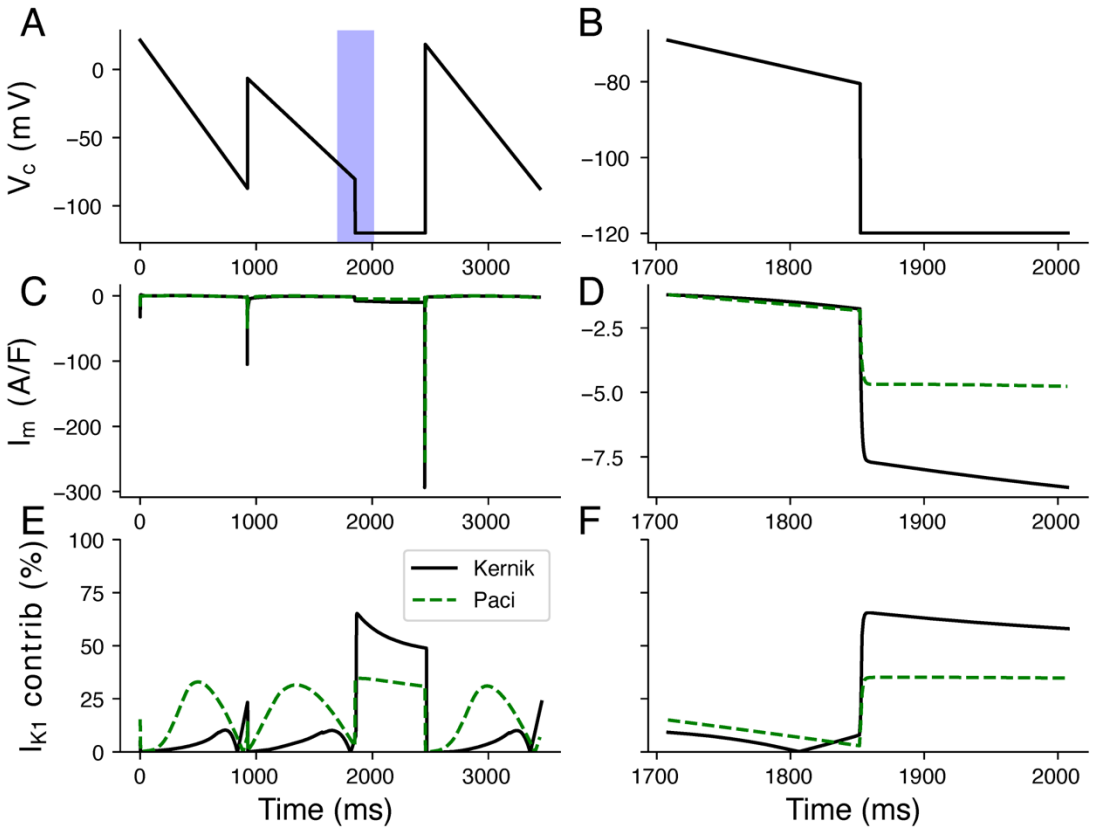


**Figure S6: The optimized protocol for $I_{K1}$ with Kernik-Clancy and Paci current responses.**

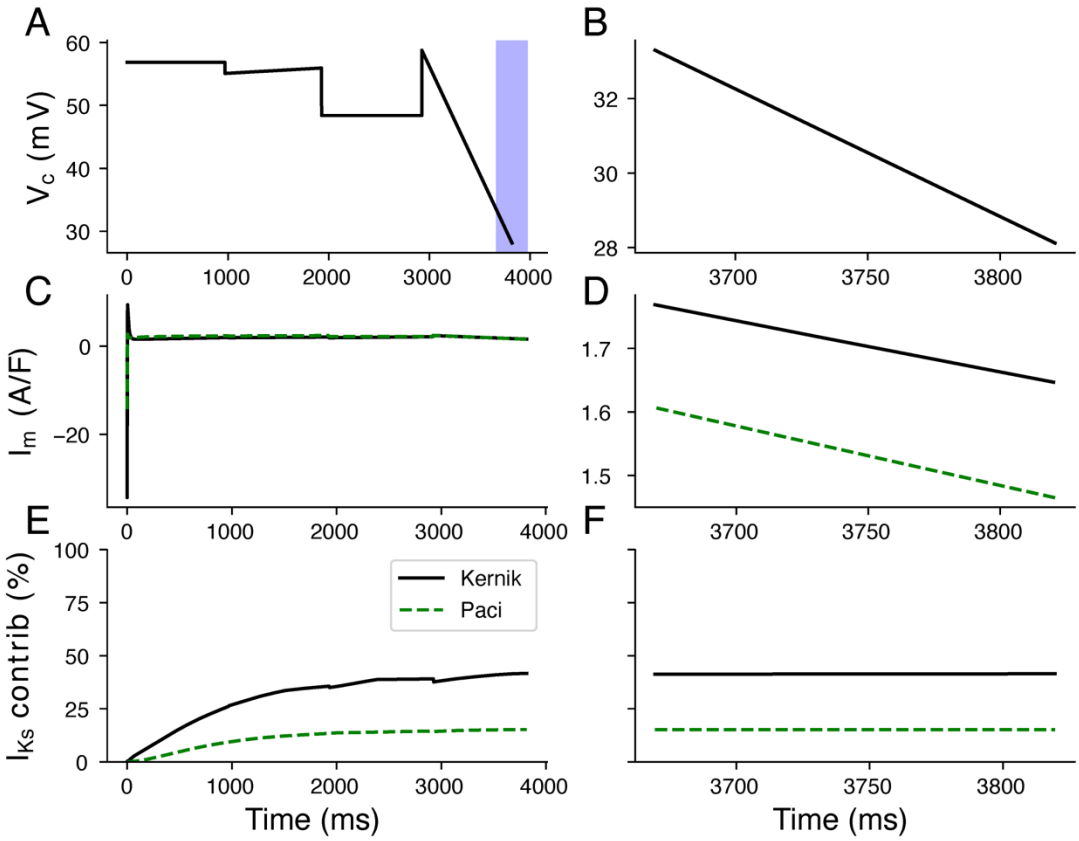


**Figure S7: The optimized protocol for $I_{Ks}$ with Kernik-Clancy and Paci current responses.**

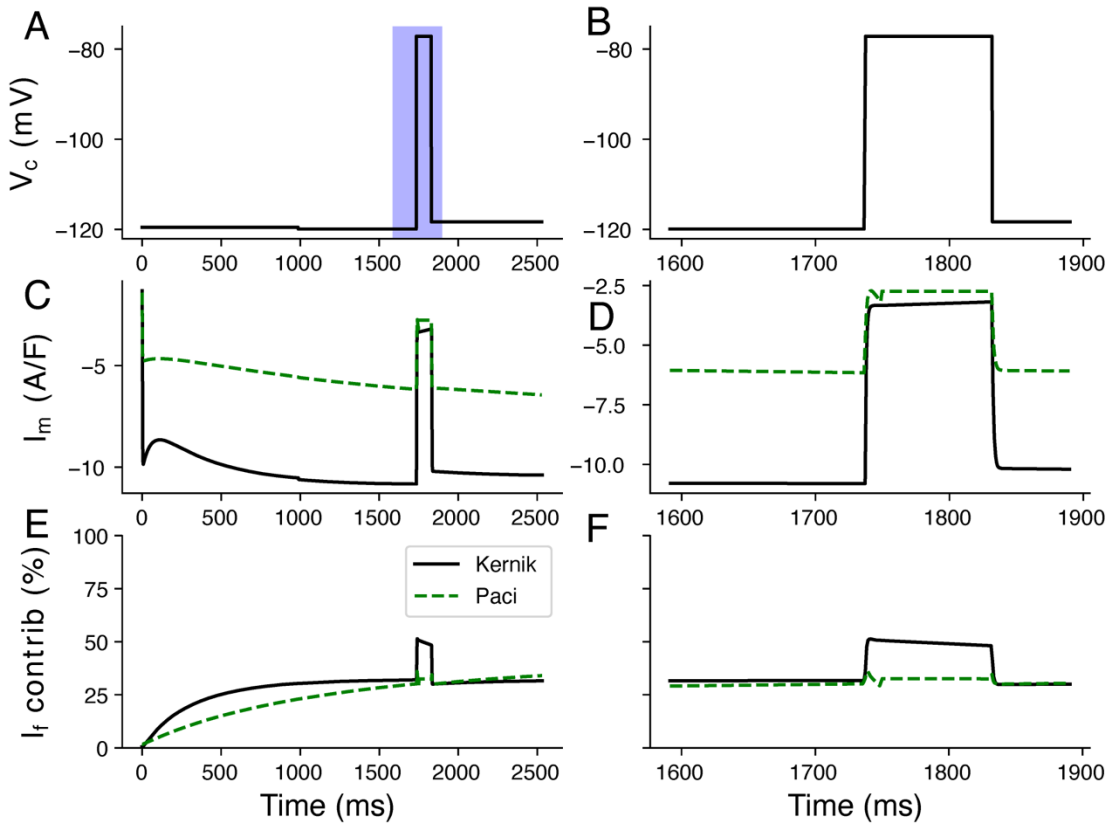


**Figure S8: The optimized protocol for $I_f$ with Kernik-Clancy and Paci current responses.**

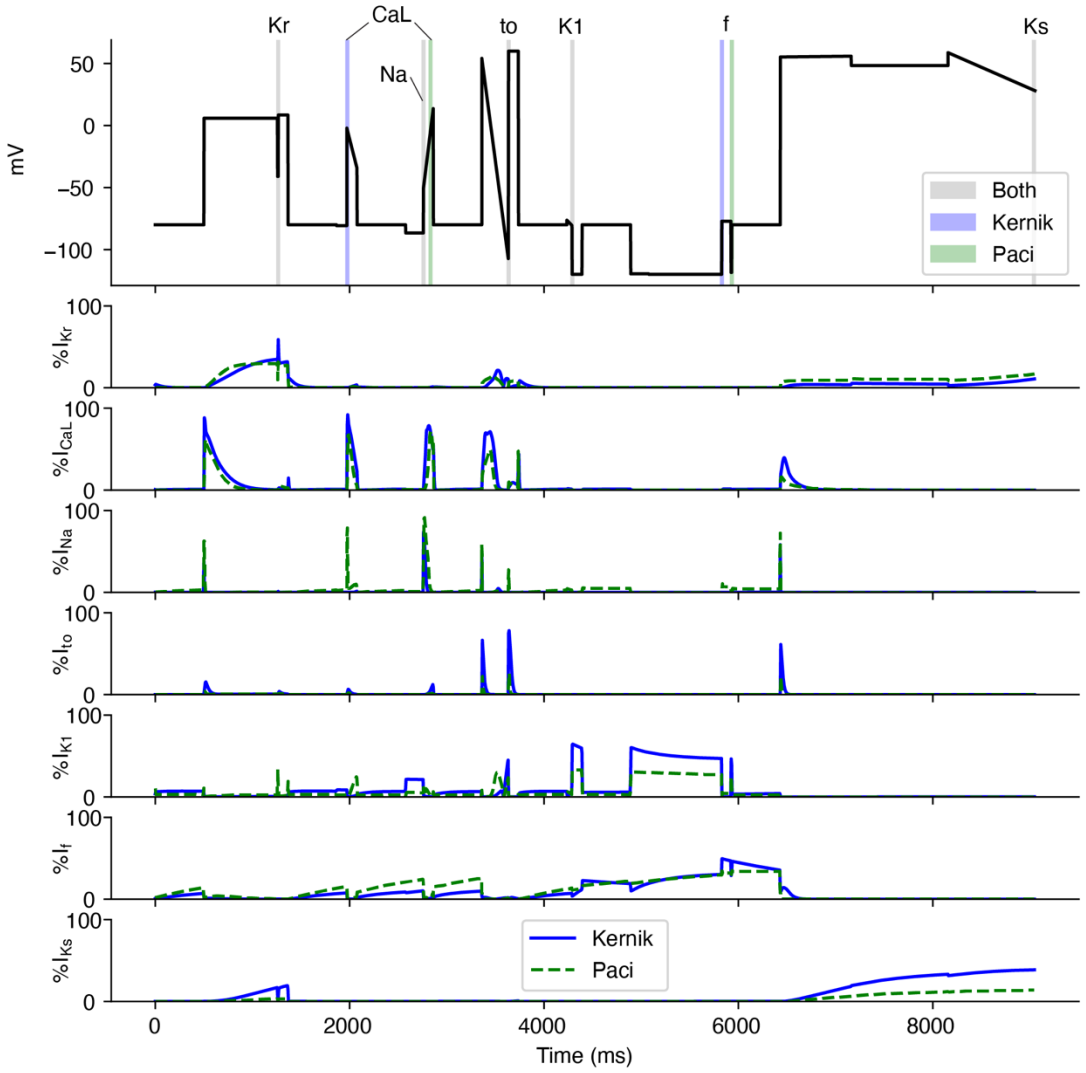


**Figure S9: The timepoints of maximum current isolation for the Paci and Kernik-Clancy models.** Five ($I_{K1}$, $I_{to}$, $I_{Kr}$, $I_{Ks}$, and $I_{Na}$) of the seven currents in the Paci model were isolated within 10 ms of when they were isolated in the Kernik-Clancy model. These time windows are highlighted grey in the top panel. The maximum $I_{CaL}$ isolation in the Paci model occurs far from where the current is maximized in the Kernik-Clancy model. However, the Paci model had a current isolation within 5% of its maximum during the Kernik-Clancy window. The timepoints for $I_f$ also differed between the two models. However, these timepoints are near one another and have similar voltage dynamics, indicating that the Kernik-Clancy timepoint is likely generalizable

for these currents. The remaining panels display the percent contribution of each of the seven currents for the Kernik-Clancy and Paci models throughout the protocol.

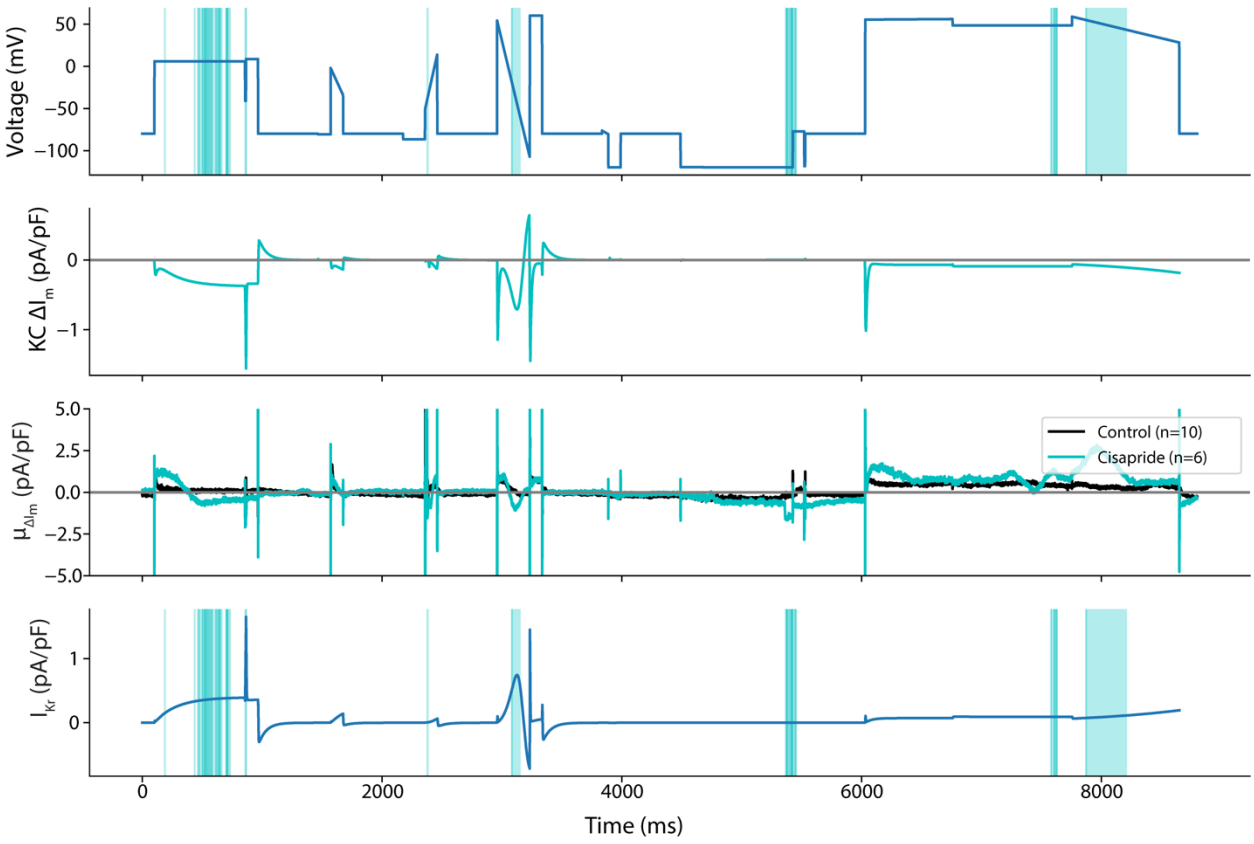


**Figure S10: Differences in cell response to cisapride vs. DMSO**. The VC protocol (panel 1), Kernik-Clancy simulated change in membrane current after cisapride treatment (panel 2), average change in experimental cell response from pre- to post-drug application for both DMSO and cisapride (panel 3), and the Kernik-Clancy $I_{Kr}$ response to the VC protocol (panel 4). The blue overlays indicate where there is a significant difference ($p<.05$) between the average cisapride and DMSO responses. We expected cisapride to strongly and specifically block $I_{Kr}$. The bottom panel shows that most of the areas that are significantly different occur when $I_{Kr}$ is present in the Kernik-Clancy model.

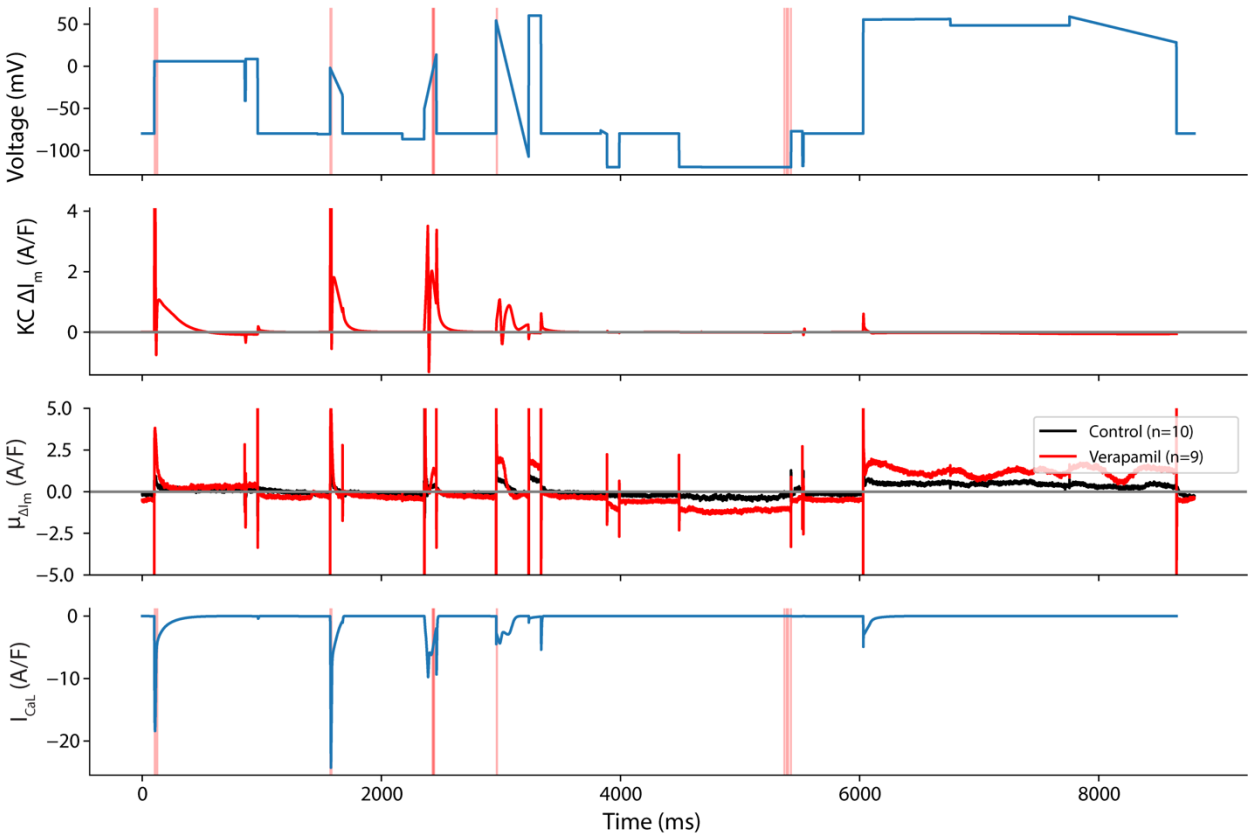


**Figure S11: Differences in cell response to verapamil vs. DMSO**. This figure shows the VC protocol (panel 1), Kernik-Clancy simulated change in membrane current after verapamil treatment (panel 2), average change in experimental cell response from pre- to post-drug application for both DMSO and verapamil (panel 3), and the Kernik-Clancy $I_{CaL}$ response to the VC protocol. The red overlays indicate where there is a significant difference ($p<.05$) between the average verapamil and DMSO responses. At the concentration tested, we expect verapamil to block ~40% of $I_{CaL}$ and ~20% of $I_{Kr}$. The bottom panel shows that most of the areas that are significantly different occur when the $I_{CaL}$ is present in the Kernik-Clancy model. There are two brief windows that the functional t-test identifies after 4000 ms, that are not likely $I_{Kr}$ or $I_{CaL}$.

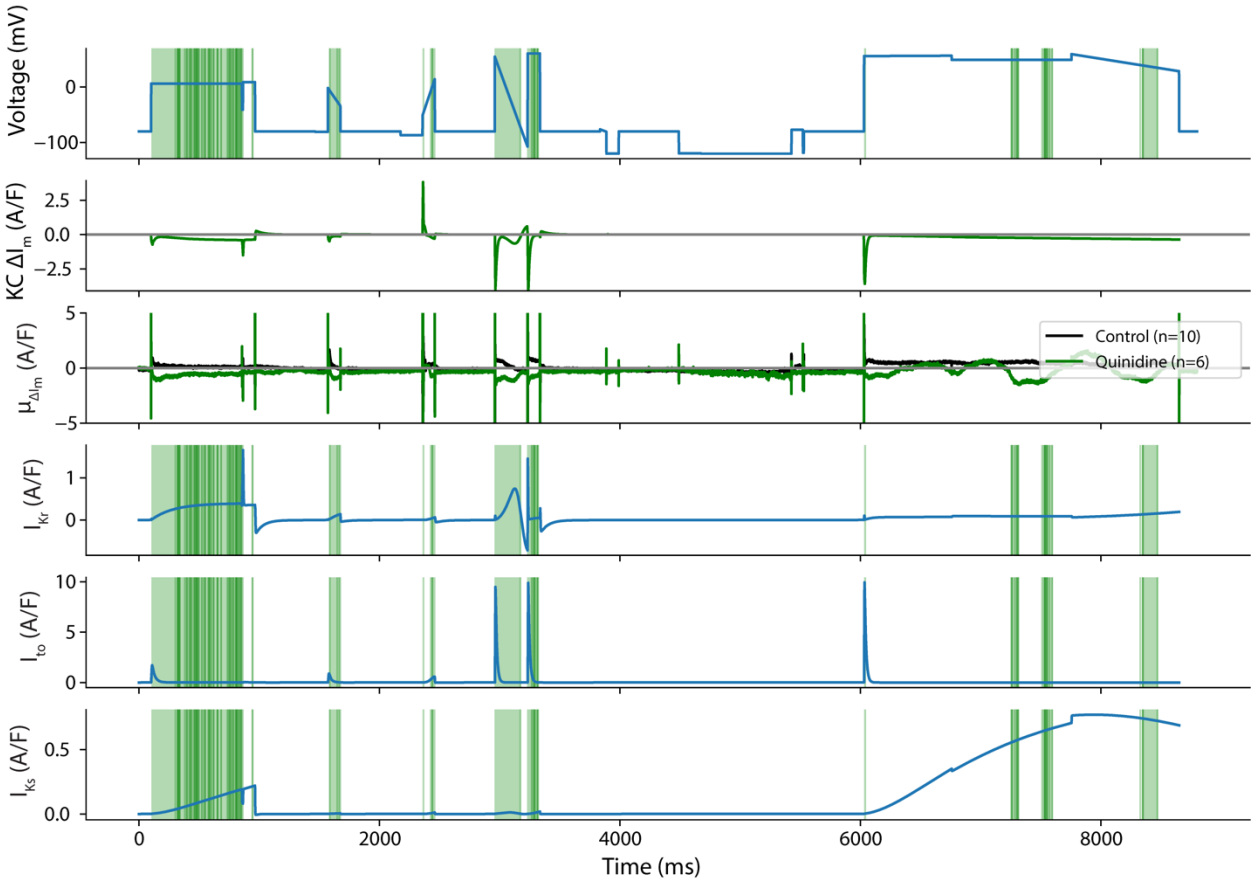


**Figure S12: Differences in cell response to quinidine vs. DMSO**. This figure shows the VC protocol (panel 1), Kernik-Clancy simulated change in membrane current after quinidine treatment (panel 2), average change in experimental cell response from pre- to post-drug application for both DMSO and quinidine (panel 3), and the Kernik-Clancy $I_{Kr}$(panel 4), $I_{to}$ (panel 5), and $I_{Ks}$ (panel 6) responses to the VC protocol. The green overlays indicate where there is a significant difference ($p<.05$) between the average quinidine and DMSO responses. At the concentration tested, we expect quinidine to block ~89% of $I_{Kr}$, ~43% of $I_{to}$, and ~27% of $I_{Ks}$. The significance windows overlap very well with the Kernik-Clancy $I_{Kr}$, $I_{to}$, and $I_{Ks}$ currents. This is to be expected, as quinidine is known to be a strong and general blocker of potassium currents.

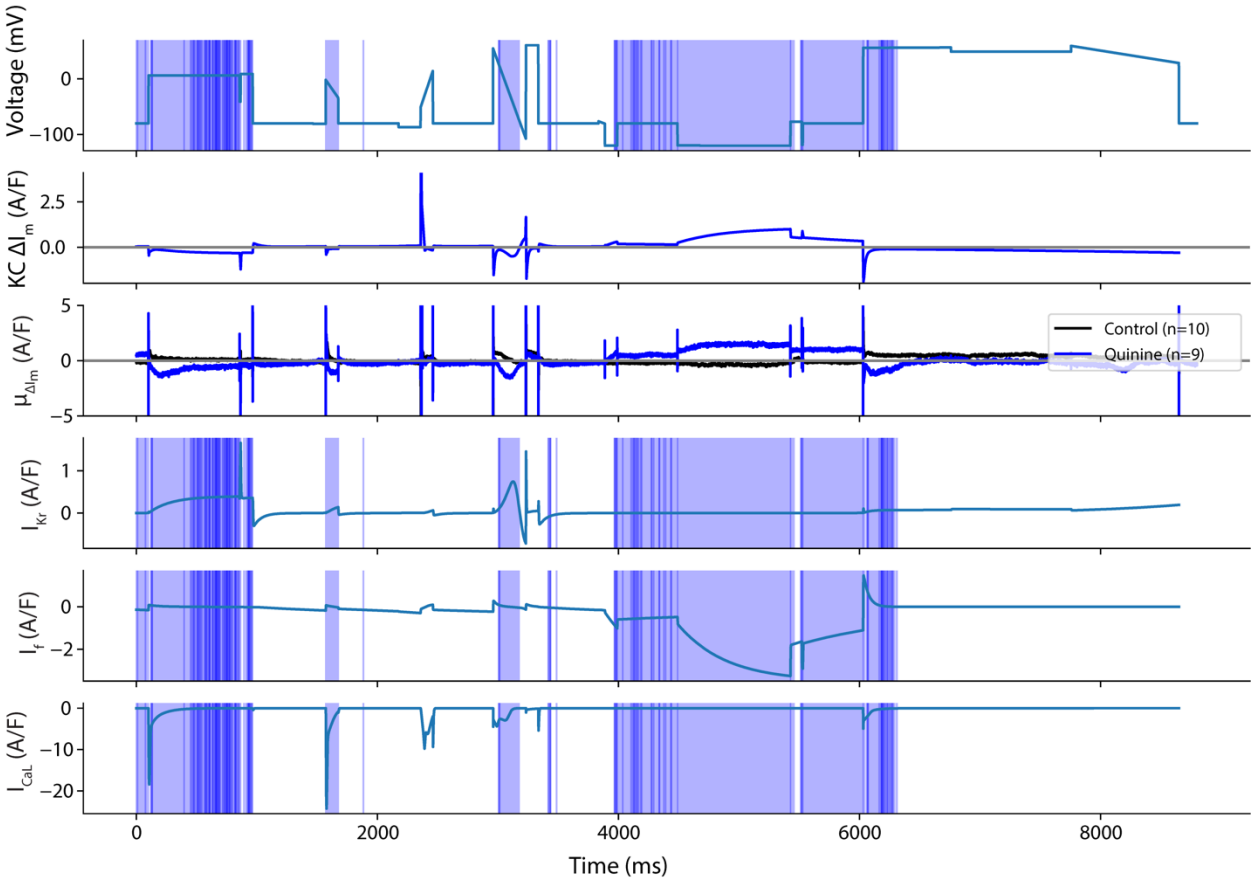


**Figure S13: Differences in cell response to quinine vs. DMSO**. This figure shows the VC protocol, Kernik-Clancy simulated change in membrane current after quinine treatment (panel 2), average change in drug response from pre- to post-drug application for both DMSO and quinidine (panel 3), and the Kernik-Clancy $I_{Kr}$ (panel 4), $I_f$ (panel 5), and $I_{CaL}$ (panel 6) responses to the VC protocol. The blue overlays indicate where there is a significant difference ($p<.05$) between the average quinine and DMSO responses. At the concentration tested, we expect quinine to block ~72% of $I_{Kr}$ and ~29% of $I_{CaL}$. During the experiments, we noticed a likely block of $I_f$ with quinine treatment. In figure 7, we show how we calculate a block of ~32% of $I_f$ by quinine at this concentration using a HEK-HCN1 cell line. The significance windows overlap very well with the Kernik-Clancy $I_{Kr}$, $I_{CaL}$, and $I_f$ currents.

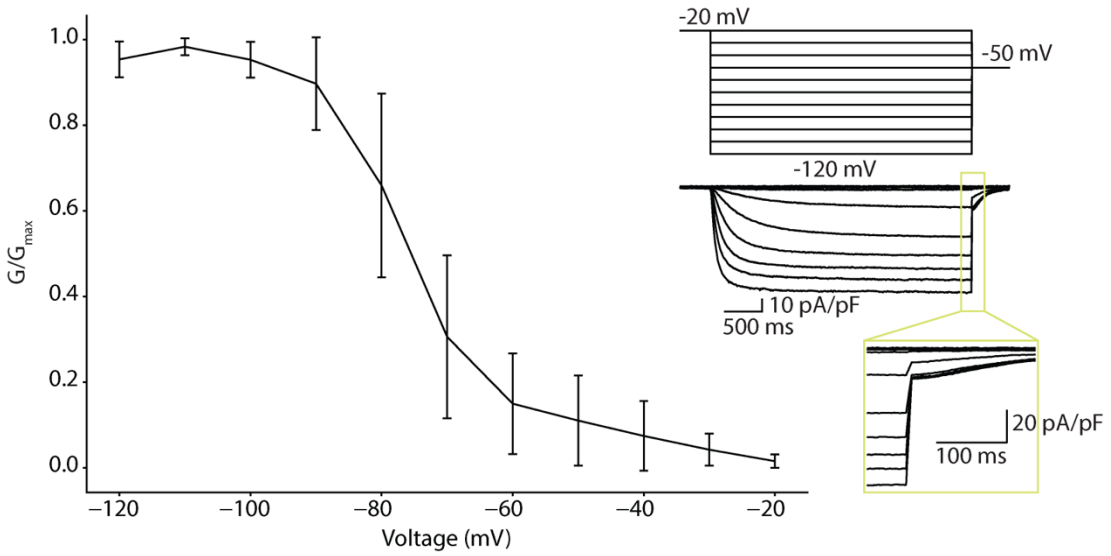


**Figure S14: Max current vs voltage for HCN1 tail current.** The max conductance-voltage curve was found by stepping to -50mV after the channels had been activated with a depolarizing step. The max tail current values in this plot indicate that most, if not all, funny current channels are open when stepping to voltages below -100mV.